

We are IntechOpen, the world's leading publisher of Open Access books Built by scientists, for scientists

6,900

Open access books available

186,000

International authors and editors

200M

Downloads

Our authors are among the

154

Countries delivered to

TOP 1%

most cited scientists

12.2%

Contributors from top 500 universities



WEB OF SCIENCE™

Selection of our books indexed in the Book Citation Index
in Web of Science™ Core Collection (BKCI)

Interested in publishing with us?
Contact book.department@intechopen.com

Numbers displayed above are based on latest data collected.
For more information visit www.intechopen.com



Electrical Conductivity, Thermoelectric Power and Crystal and Band Structures of EDOB-EDT-TTF Salts Composed of PF_6^- , AsF_6^- and SbF_6^-

Tomoko Inayoshi

Additional information is available at the end of the chapter

<http://dx.doi.org/10.5772/65561>

Abstract

Novel 2:1 EDOB-EDT-TTF radical salts with different octahedral PF_6^- , AsF_6^- , and SbF_6^- anions were prepared by electrochemical oxidation. AsF_6^- salt was found to be isostructural to PF_6^- salt and had a triclinic crystal structure, while SbF_6^- salt was not isostructural with PF_6^- salt and had monoclinic crystal structure. PF_6^- salt had higher metal-to-semiconductor (MS) transition temperature, than that of AsF_6^- salt, while SbF_6^- salt exhibited semiconductive behavior throughout the temperature range of electrical conductivity measurements. To clarify MS transition of these salts, thermoelectric power measurements were also carried out. Thus, thermoelectric power apparatus was constructed and measurements were performed simultaneously with thermoelectric power and electrical resistivity measurements. Crystal structural features for EDOB-EDT-TTF salts at 90, 293, 330 and 350 K, as well as conductivity, thermoelectric power measurements and band structures before and after MS transition are described.

Keywords: EDOB-EDT-TTF radical salts, conductivity, thermoelectric power

1. Introduction

Highly conducting organic TTF·TCNQ complex composed of tetrathiafulvalene (TTF) and tetracyanoquinodimethane (TCNQ) was reported by Heeger et al. in 1973 [1] and has been studied by many physicists and chemists as a one-dimensional conducting system [2, 3]. TTF·TCNQ provides highly anisotropic charge-transfer (CT) complex with metallic properties down to 58 K along *b*-axis, in which crystal structure [4] has two columns of TTF and TCNQ. Thermoelectric power of TTF·TCNQ along *b*-axis is negative and proportional to absolute

temperature down to 140 K, but not along *a*-axis [5]. This is consistent with electrical conductivity measured along different axes. Apparatus for thermoelectric power measurement on organic single crystals has been reported by Chaikin and Kwak [6]. It is designed specifically for small fragile anisotropic samples, such as TCNQ salts. Measurements can be taken with a small (0.5 K) temperature gradient for good temperature resolution.

Bis(ethylenedithio)tetrathiafulvalene (BEDT-TTF) is a good electron donor, and CT complexes and radical salts composed of BEDT-TTF also grow excellent crystals. BEDT-TTF radical salts afford many superconductors as two-dimensional conducting system. In the case of such two-dimensional system, thermoelectric power often exhibits complicated temperature dependence and anisotropy. Mori and Inokuchi have found an agreement between thermoelectric power and calculations for β -(BEDT-TTF)₂I₃ and κ -(BEDT-TTF)₂Cu(NCS)₂ [7].

Bis(ethylenedioxy)dibenzotetrathiafulvalene (BEDO-DBTTF) modified with strong electron-donating groups containing ethylenedioxy groups has been synthesized [8]. BEDO-DBTTF CT complexes and salts afforded no metallic compounds. Therefore, we have synthesized a new unsymmetrical EDOB-EDT-TTF donor, which consists of parts of BEDO-DBTTF and BEDT-TTF, and EDOB-EDT-TTF radical salts with octahedral PF₆⁻, AsF₆⁻, and SbF₆⁻ anions [9, 10]. Based on electrical resistivity measurements, PF₆ and AsF₆ salts underwent a metal-to-semiconductor (MS) transition. X-ray analyses of these salts elucidated their crystal characteristics. Simultaneous measurements of thermoelectric power and electrical resistivity on a single sample were performed for these salts. MS transition temperatures of these PF₆ and AsF₆ salts were also determined from their thermoelectric power.

2. Preparation of organic conductors

2.1. Synthesis of unsymmetrical EDOB-EDT-TTF donor

As shown in **Figure 1**, synthesis of EDOB-EDT-TTF was carried out using two synthetic methods: cross-coupling (I) and thermal decomposition (II), resulting in 30 and 27% yields, respectively.

2.1.1. Cross-coupling method

To the suspension of **1** (3.0 g, 12 mmol) and **2** (2.5 g, 12 mmol) in dry benzene (40 mL) was added triethyl phosphate (30 mL, 130 mmol). The mixture was refluxed for 5 h at 80°C. The resulting orange precipitate was removed by filtration, and the filtrate was purified by silica gel column chromatography using CHCl₃/hexane (5:1) as the eluent. The second fraction was collected, and the resulting product was recrystallized using ethyl acetate to afford EDOB-EDT-TTF as orange crystals (30% yield): mp 260–262. ¹H NMR (CDCl₃): δ 3.30 (4H, s, -SCH₂), 4.23 (4H, s, -OCH₂), 6.77 (2H, s, ArH). MS (EI) *m/z*: 402 (M⁺). IR (KBr, ν_{\max} cm⁻¹): 1575 (w), 1540 (w), 1478 (s), 1456 (s), 1300 (s), 1376 (m), 1360 (m), 1100 (m), 1063 (s), 908 (m), 895 (m), 854 (m), 772 (w). UV-vis (CHCl₃) λ_{\max} nm: 454, 344, 313, > 260. Anal. calcd for C₁₄H₁₀O₂S₆: C, 41.77; H,

2.50; S, 47.78. Found: C, 41.77; H, 2.47; S, 47.74. The product was subsequently subjected to X-ray crystal structure analysis.

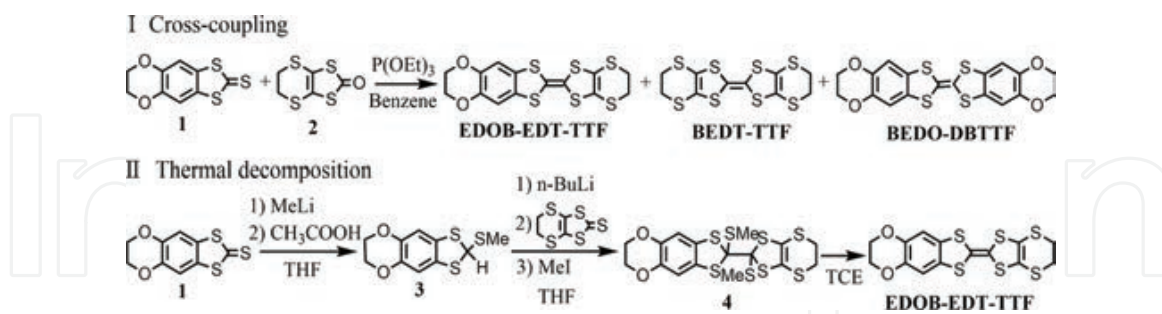


Figure 1. Synthetic routes of EDOB-EDT-TTF.

2.1.2. Thermal decomposition method

2-(Methylthio)-5,6-ethylenedioxy-1,3-benzodithiole (3). To a solution of **1** (1.03 g, 4.25 mmol) in dry THF (150 mL) at -78°C under nitrogen was added solution of MeLi (5.1 mL, 6 mmol) dropwise via a syringe. After stirring for 5 h, the mixture was treated with acetic acid (2 mL) and allowed to warm to room temperature. The mixture was combined with water, and the desired compound was extracted using CH_3Cl . The organic layer was dried using MgSO_4 and evaporated *in vacuo* to afford the crude product, which was purified using silica gel chromatography with tetrahydrofuran THF/*n*-hexane (1:3) as the eluent to afford **3** as a colorless oil (0.74 g, 66%). $^1\text{H NMR}$ (CDCl_3): δ 2.22 (3H, s, $-\text{SCH}_3$), 4.21 (4H, s, $-\text{OCH}_2$), 5.93 (1H, s, $-\text{CH}$), 6.79 (2H, s, ArH). HRMS (EI) (*m/z*): calcd for $\text{C}_{10}\text{H}_{10}\text{O}_2\text{S}_2$, 257.9843; found, 257.9718.

Hexathioorthooxalate (4). To a stirred solution of **3** (2.60 g, 10 mmol) in dry THF (120 mL) at -78°C under nitrogen was added *n*-BuLi (6.35 mL, 9.5 mmol) dropwise using a syringe. After stirring for 1 h, 4,5-ethylenedithio-1,3-dithiol-2-thione (2.24 g, 10 mmol) in THF was added dropwise to the mixture, followed by addition of an excess of MeI (1.91 mL, 30 mmol) via a syringe to the mixture after 1 h. After further stirring for 1 h, the solution was treated with portions of 1 mol/dm^3 aq. NH_4Cl . The mixture was allowed to warm to room temperature, and the aqueous layer was extracted with CH_2Cl_2 . The organic phase was concentrated and purified using silica gel column chromatography with $\text{CH}_3\text{Cl}/n$ -hexane (1:2) as the eluent to afford **4** as a yellow solid (2.40 g, 45%): mp $207\text{--}213$ (dec. 150°C); $^1\text{H NMR}$ (CDCl_3): δ 2.46 (3H, s, $-\text{SCH}_3$), 2.53 (3H, s, $-\text{SCH}_3$), 3.25 (4H, m, $-\text{SCH}_2$), 4.21 (4H, s, $-\text{OCH}_2$), 6.62 (2H, s, ArH). Anal. calcd for $\text{C}_{16}\text{H}_{16}\text{O}_2\text{S}_8$: C, 38.68; H, 3.25. Found: C, 38.56; H, 3.17.

EDOB-EDT-TTF. After refluxing **4** in 1,1,2-trichloroethane (TCE) for 12 h, the crude product was purified by column chromatography with $\text{CH}_2\text{Cl}_2/n$ -hexane (1:1) as the eluent followed by recrystallization from ethyl acetate to yield EDOB-EDT-TTF (27%). $^1\text{H NMR}$ and MS data were comparable to those obtained by the cross-coupling method.

The redox potentials of unsymmetrical EDOB-EDT-TTF appeared middle between that of BEDT-TTF and BEDO-DBTTF, as similar to other unsymmetrical TTF derivatives reported in [11]. The difference potential (ΔE) between the first redox potential ($E_{1/2(1)}$) and the second redox

potential ($E_{1/2(2)}$) is related to intramolecular on-site Coulomb repulsion energy, U . The ΔE of EDOB-EDT-TTF also showed middle between that of BEDT-TTF and BEDO-BDTTF. The U of EDOB-EDT-TTF decreased compared to that of BEDO-BDTTF.

2.2. Preparation of CT complexes and radical salts

Hot solutions of each donor and acceptor in acetonitrile were mixed. After the reaction mixture was cooled to room temperature (RT), the resulting precipitate was collected by filtration. Complexes were washed with the same organic solvent and dried *in vacuo*. Black octahedral PF_6 , AsF_6 and SbF_6 salts were obtained by electrochemical oxidation in distilled 1,2-dichloroethane or TCE under constant current of 1 μA in a mixture of the donor and the tetra-*n*-butylammonium salts of the corresponding anions at RT using H-shaped cell with Pt electrodes for 2 weeks. Stoichiometry of CT complexes and radical salts was determined using elemental analysis or X-ray crystallographic analyses.

3. Measurements

3.1. Electrical conductivity measurement

DC conductivities were measured with standard four- or two-probe techniques, using Keithley 220 current source, Keithley 199 voltage/scanner, Keithley 195A voltmeter, and Scientific Instruments 9650 temperature controller. For powder samples, measurements were performed on compressed pellets, which were cut to form orthorhombic shape. Gold wires were glued to the samples with gold paint (Tokuriki Chemical, no. 8560).

3.2. Apparatus for simultaneous measurements of thermoelectric power and resistivity on organic conductors

Simultaneous measurements of thermoelectric power and resistivity by a two-probe method of PF_6 , AsF_6 , and SbF_6 salts were performed using computer-interfaced system, which schematic diagram is shown in **Figure 2**.

Software program for controlling the system was created in LabVIEW by Computer Automation Co. and System Approach Co. By applying different digital signals using relay and counter timer, we could perform simultaneous measurements of thermoelectric power and two-probe electrical resistivity on a single sample over the entire temperature range [12]. First, by opening the circuit through Keithley 2002 multimeter attached 2001-Scan scanner card as the relay, sample voltage (ΔV) between V^+ and V^- electrodes was measured by Keithley 2182 nanovoltmeter. Temperature gradient, ΔT , between two copper plates was measured by another Keithley 2182 nanovoltmeter. Thermoelectric power was determined. Second, after thermal equilibrium was sufficiently reached between two copper plates, by connecting the circuit through the relay, sample voltage was measured by Keithley 2182 nanovoltmeter, while constant current was supplied to the sample reversing leads to cancel thermal EMFs by Keithley 220 current source. Two-probe resistance measurement was determined by subtract-

ing these two voltages and averaging. Using thermoelectric power stage made by MMR Technologies Inc. radical salts and the reference Cu-constantan or Au/Fe-Chromel thermocouple wire were glued onto copper plates using gold paint. Thermal gradient across the sample was applied by heating chip resistor (110 Ohm), which was applied from loop 2 of LakeShore 331S temperature controller. Thermoelectric power was determined from the slope of the line and was calculated as follows: $S = \Delta V / \Delta T$ [13], where ΔT of 15 total points was typically < 0.5 K. Changing voltage value was measured at specific fixed time intervals by 15 points simultaneously using different nanovoltmeters. Therefore, it is necessary to apply synchronously digital signals to two Keithley 2182 nanovoltmeters. By using National Instruments PCI-6602 counter timer, we could measure 15 points synchronously to determine ΔV and ΔT . It was necessary to subtract the offset drift in order to obtain absolute thermoelectric power of the samples. At each measurement, temperature of the sample holder in the cryostat was controlled using loop 1 of LakeShore 331S temperature controller with sensor (DT-470). System was checked by measurements with Pt standard [14] and TTF·TCNQ complex [5, 15] in temperature range 4–350 K.

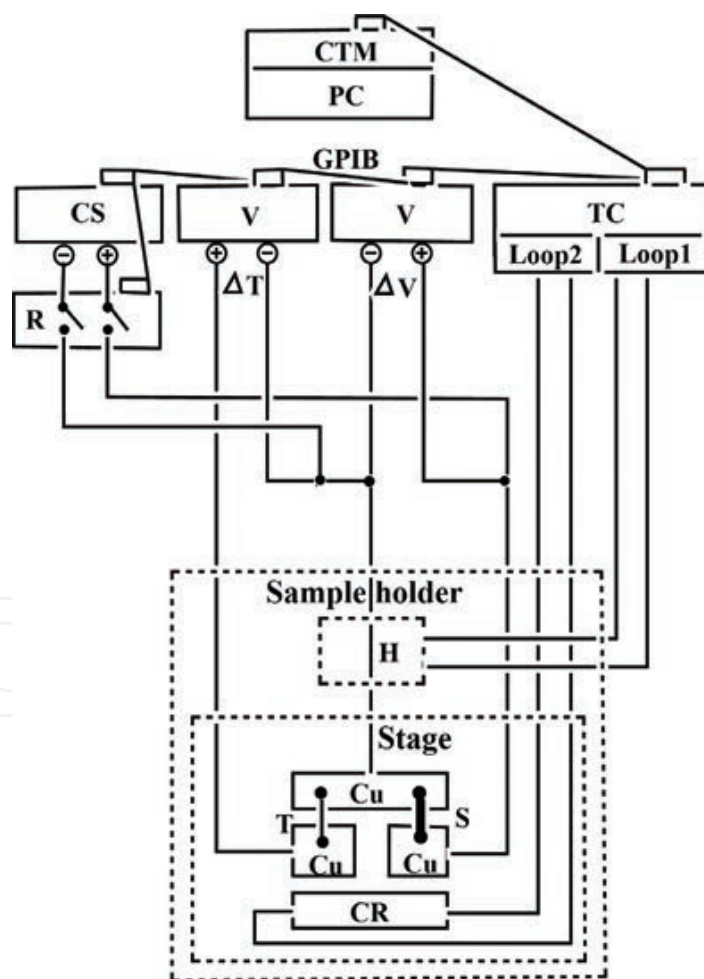


Figure 2. Schematic diagram for simultaneous measurements of thermoelectric power and two-probe electrical resistivity. CTM: counter timer 6602; TC: temperature controller 331S; V: nanovoltmeter 2182; CS: current source 220; R: relay 2002; H: heater; S: sample; T: thermocouple wire; CR: chip resistor.

Simultaneous measurements of thermoelectric power and resistivity of (EDOB-EDT-TTF)₂PF₆ were also performed on Quantum Design PPMS Model P670 Thermal Transport System (TTO) in temperature range 232-327 K. The crystal, which was glued to two-probe using bar-shaped copper leads, was mounted on a TTO sample puck.

4. Crystal structure

Single crystal structure analyses have been carried out for PF₆ salt at 298 K, AsF₆ salt at 90, 293, 330, and 350 K, SbF₆ salt at 90 and 293 K. Crystallographic data are listed in **Table 1**.

	PF ₆ salt at 298 K	AsF ₆ salt at 90 K	AsF ₆ salt at 293 K	AsF ₆ salt at 330 K	AsF ₆ salt at 350 K	SbF ₆ salt at 90 K	SbF ₆ salt at 293 K
Chemical formula	C ₂₈ H ₂₀ F ₆ O ₄ PS ₁₂		C ₂₈ H ₂₀ AsF ₆ O ₄ S ₁₂			C ₂₈ H ₂₀ F ₆ O ₄ S ₁₂ Sb	
Formula weight	950.23		994.15			1040.99	
Crystal system	Triclinic		Triclinic			Monoclinic	
Space group	<i>P</i> -1		<i>P</i> -1			<i>C</i> 2/ <i>c</i>	
<i>a</i> /Å	7.003	6.875	7.000	7.036	7.057	37.805	38.105
<i>b</i> /Å	8.074	7.914	8.061	8.092	8.112	8.204	8.340
<i>c</i> /Å	16.326	16.411	16.424	16.411	16.404	11.371	11.429
<i>α</i> /°	76.02	103.40	76.07	76.23	76.34		
<i>β</i> /°	78.07	98.34	78.41	78.46	78.49	103.23	102.77
<i>γ</i> /°	81.50	97.11	81.45	81.07	80.85		
<i>V</i> /Å ³	871.7	847.8	876.2	883.4	888.0	3433.0	3542.4
<i>Z</i>	1	1	1	1	1	4	4
<i>T</i> /K	298	90	293	330	350	90	293
CCDC no.		819768	809939	809703	802121	799928	799214

Table 1. Crystallographic data for EDOB-EDT-TTF salts.

4.1. Crystal structure of (EDOB-EDT-TTF)₂PF₆

Crystal structure of 2:1 (EDOB-EDT-TTF)₂PF₆ at 298 K is depicted in **Figure 3** and belongs to triclinic *P*-1 space group. Cation layers of EDOB-EDT-TTF molecules and anion layers of PF₆⁻ anions are arranged alternately along the direction of *a*-axis. Donor molecules in the crystal are stacked in alternating orientations along the stacking axis. Average interplanar donor-donor distances in the columns equal to 3.635 and 3.641 Å, respectively. This donor packing arrangement is so-called *β*-type structure [16] as in *β*-(BEDT-TTF)₂I₃ [17]. Intermolecular side-by-side short contacts, less than van der Waals (vdW) [18] sum, are observed at S(6)...S(6) (3.55 Å: vdW sum = 3.60 Å) and O(1)...H(11A) (2.63 Å: vdW sum = 2.72 Å). Intermolecular intrastack

short contacts O(1)...H(5A) (2.693 Å) and C(8)...H(4A) (2.756 Å; vdW sum = 2.90 Å) are alternatively found along *b*-axis. Intermolecular S...F short contacts less, than vdW sum (3.27 Å for S...F) between EDOB-EDT-TTF cations and hexafluorophosphate anions, are not observed. Octahedral anion does not show rotational disorder.

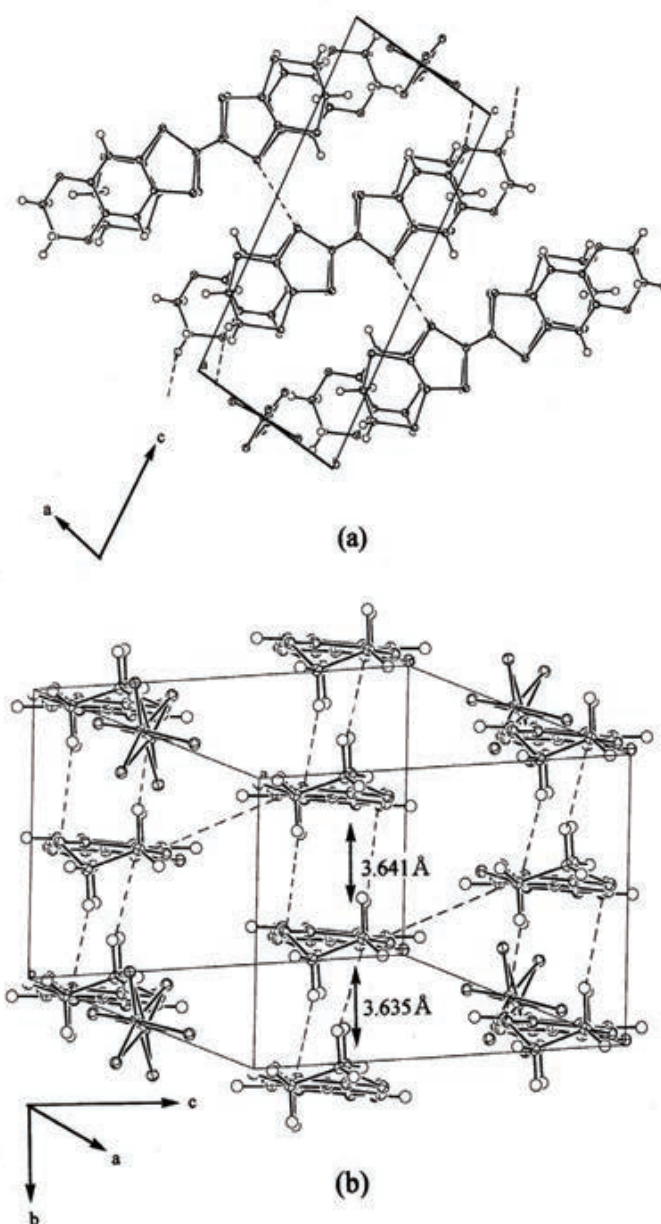


Figure 3. Crystal structure of (EDOB-EDT-TTF)₂PF₆: (a) viewed along *b*-axis and (b) viewed along molecular long axis. Broken lines represent intermolecular short contacts.

4.2. Crystal structure of (EDOB-EDT-TTF)₂AsF₆

Crystal structure of (EDOB-EDT-TTF)₂AsF₆ is isostructural to PF₆ salt and was elucidated at various temperatures (90, 293, 330 and 350 K). Cation layers of donor molecules and anion layers of AsF₆⁻ anions are arranged alternately along the direction of *c*-axis as shown in

Figure 4. EDOB-EDT-TTF molecules are packed head-to-tail in face-to-face overlapping manner and alternately stacked with different interplanar along *b*-axis. There are intermolecular short S...S, O...H and S...F contacts, less than vdW sum. Interstack S(1)...S(1) short contacts less than 3.60 Å, are observed over the entire temperature range (3.530 Å at 90 K, 3.548 Å at 293 K, 3.555 Å at 330 K, and 3.563 Å at 350 K), and S(3)...S(6) short contacts are found at 90 K (3.536 Å), but not at 293 K (3.629 Å), 330 K (3.654 Å), and 350 K (3.669 Å). S...S short contacts are found only between the stacks and not within the stacks. Side-by-side O(2)...H(6B)–C(6) short contacts (2.673 Å at 90 K, 2.647 Å at 293 K, 2.637 Å at 330 K, and 2.634 Å at 350 K), less than vdW sum in intermolecular interstack along *c*-axis, are observed over the entire temperature range as shown in **Figure 4**. O(2)...H(12A)–C(12) short contacts in intermolecular intrastack along *b*-axis (**Figure 4a**) can be seen at 90 K (2.440 Å), 293 K (2.610 Å) and

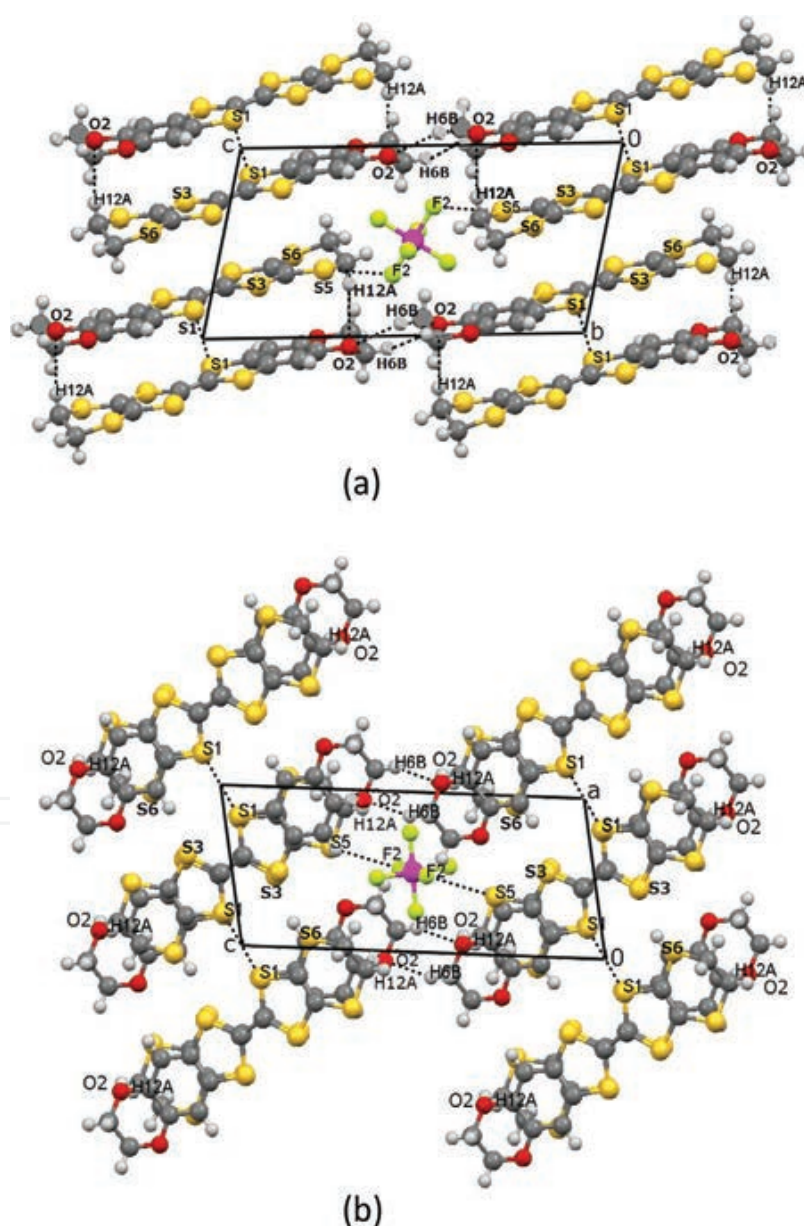


Figure 4. Crystal structure of (EDOB-EDT-TTF)₂AsF₆ at 293 K showing short contacts as dashed lines: (a) projection in *bc* plane and (b) projection in *ac* plane.

330 K (2.721 Å), but not at 350 K (2.757 Å). Only O(2)...H(12A)–C(12) short contacts exist within the intermolecular intrastack dimer. The other O(2)...H(6B), S...S, and S...F short contacts exist in the intermolecular interstack along the transverse direction. Owing to the effect of dimerization, distances of O(2)...H(12A)–C(12) at 90, 293, and 330 K are shorter than those at 350 K. Intermolecular S(5)...F(2) short contacts, less than vdW sum between EDOB-EDT-TTF cations and hexafluoroarsenate anions, are observed at 90 K (3.080 Å), 293 K (3.208 Å), and 330 K (3.255 Å), but not at 350 K (3.279 Å). Octahedral anion does not show rotational disorder.

4.3. Crystal structure of (EDOB-EDT-TTF)₂SbF₆

(EDOB-EDT-TTF)₂SbF₆ crystallizes in two forms, plate and needle. Needle form is too much small for X-ray crystal structure analysis. Crystal structure of plate (EDOB-EDT-TTF)₂SbF₆ is not isostructural to AsF₆ and PF₆ salts and belongs to monoclinic *C2/c* space group, which was elucidated at 90 and 293 K. Crystal structure of plate form at 293 K is shown in **Figure 5**, and octahedral SbF₆[−] anion does not show a disorder. Molecular arrangement of EDOB-EDT-TTF molecules is quite different from that in (EDOB-EDT-TTF)₂AsF₆. Two EDOB-EDT-TTF molecules are paired with molecular planes almost parallel, and adjacent pairs are nearly perpendicular to each other. This type of molecular arrangement tends to create two-dimensional networks [19]. However, SbF₆ salt is semiconductor. Intermolecular short S...S and O...H contacts are observed, but no S...F contacts are found at 293 and 90 K. S...S short contacts at 293 K are between S(4)...S(5) (3.502 Å) and S(5)...S(6) (3.519 Å) as shown in **Figure 5**. S...S short contacts at 90 K are seen at S(3)...S(6) (3.462 Å) and S(5)...S(6) (3.467 Å) and at S(2)...S(3) (3.563 Å) as shown in **Figure 6**. Dimerization of two EDOB-EDT-TTF molecules becomes stronger at 90 K. O...H short contacts are observed at O(2)...H(13B) (2.607 Å) (along *b*-axis) and O(2)...H(3) (2.470 Å) (along *c*-axis) at 293 K and O(1)...H(12A) (2.503 Å) (along *b*-axis) and O(1)...H(8) (2.425 Å) (along *c*-axis) at 90 K as shown in **Figures 5** and **6**.

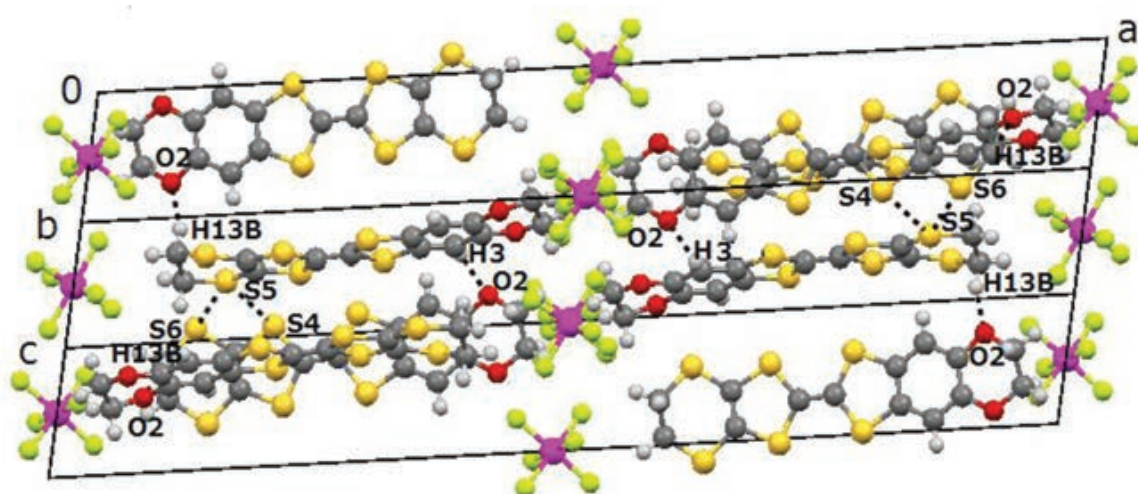


Figure 5. Crystal structure of plate (EDOB-EDT-TTF)₂SbF₆ at 293 K showing intermolecular short O...H and S...S contacts as dotted lines.

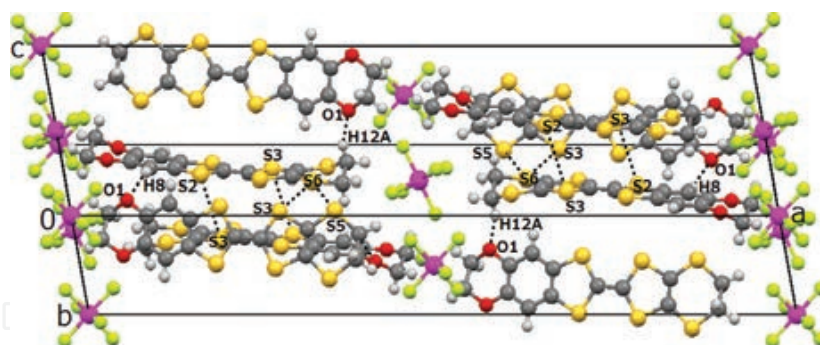


Figure 6. Crystal structure of plate (EDOB-EDT-TTF)₂SbF₆ at 90 K showing intermolecular short H...H and S...S contacts as dotted lines.

5. Electrical conductivity

Table 2 summarizes appearances, component ratios, metal-to-semiconductor (MS) transition, room-temperature electrical conductivity, and activation energies of EDOB-EDT-TTF complexes and salts. A newly [10] and the previously [9] reported (EDOB-EDT-TTF)₂PF₆ salts exhibited electrical resistivity decrease with heating (**Figure 7**) and showed resistivity minimum at 340 K, then gradual increase up to 350 K. As shown in **Figure 8**, new black plates (EDOB-EDT-TTF)₂AsF₆ ($\sigma_{RT} = 2.6 \text{ S cm}^{-1}$) exhibited distinct minimum in resistivity at 315 K confirming MS transition at this temperature. The semiconductive region ($< 315 \text{ K}$) showed the activation energy of $E_a = 0.13 \text{ eV}$. It was found that T_{MS} decreased with increase in anion size, as well as β -(BEDT-TTF)₂X (X = PF₆ and AsF₆) [20, 21]. Electrical conductivity of new black plate and fine needle SbF₆ salts at room temperature was $4.4 \times 10^{-2} \text{ S cm}^{-1}$ ($E_a = 0.13 \text{ eV}$) and $2.9 \times 10^{-3} \text{ S cm}^{-1}$ ($E_a = 0.13 \text{ eV}$), respectively. SbF₆ salts behaved as semiconductors from room temperature to 100 K.

Acceptor or anion	Appearance	Stoichiometry D:A	T_{MS}/K	$\sigma_{RT}/\text{S cm}^{-1}$	E_a/eV	References
M ₂ TCNQ	Black powder	1:1		Insulator ^a		[9]
TCNQ	Black powder	1:1		1.9 ^a	0.085	[9]
FTCNQ	Dark green powder			9.6×10^{-2a}	0.13	[9]
F ₂ TCNQ	Dark green powder	4:1		7.1×10^{-2a}	0.13	[9]
PF ₆ ⁻	Black plate	2:1	340	1.7×10^b	0.23	[9]
PF ₆ ⁻	Black plate	2:1	337	1.0 ^c	0.17	[10]
AsF ₆ ⁻	Black plate	2:1	315	2.6 ^c	0.13	[10]
SbF ₆ ⁻	Black plate	2:1		4.4×10^{-2c}	0.13	[10]
SbF ₆ ⁻	Black fine needle	2:1		2.9×10^{-3c}	0.13	[10]

^aMeasured on a compressed pellet by a four-probe method.

^bby a four-probe method.

^cby a two-probe method.

Table 2. Electric conductivities of EDOB-EDT-TTF complexes and salts.

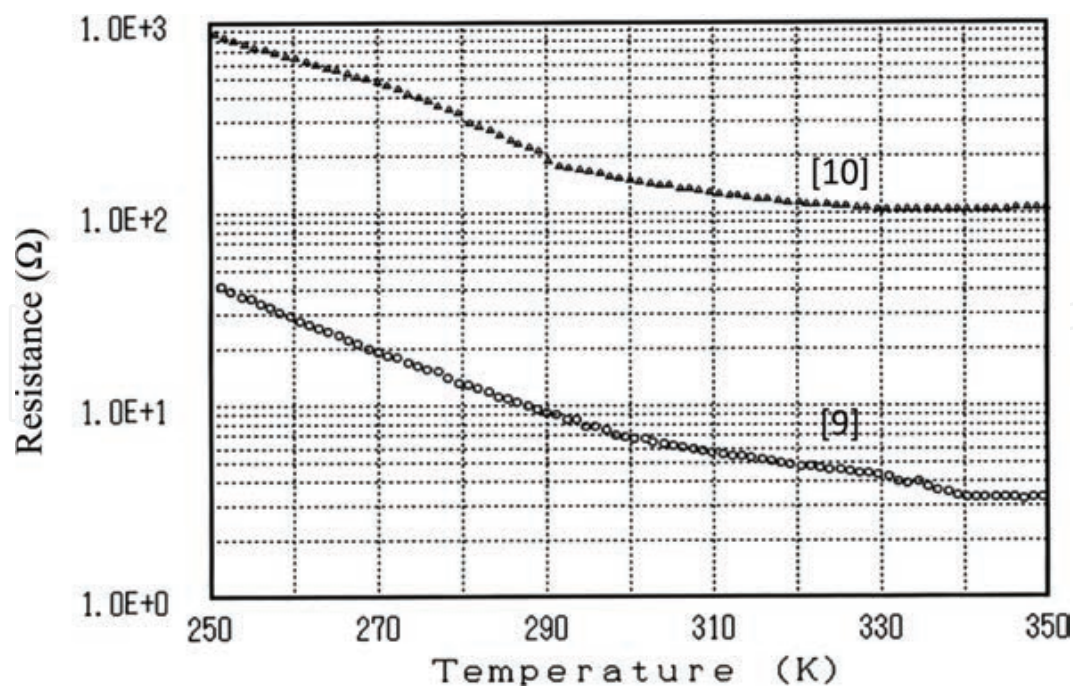


Figure 7. Temperature dependence of resistance of single crystals (EDOB-EDT-TTF)₂PF₆ in the heating run. Data for two crystals are plotted.

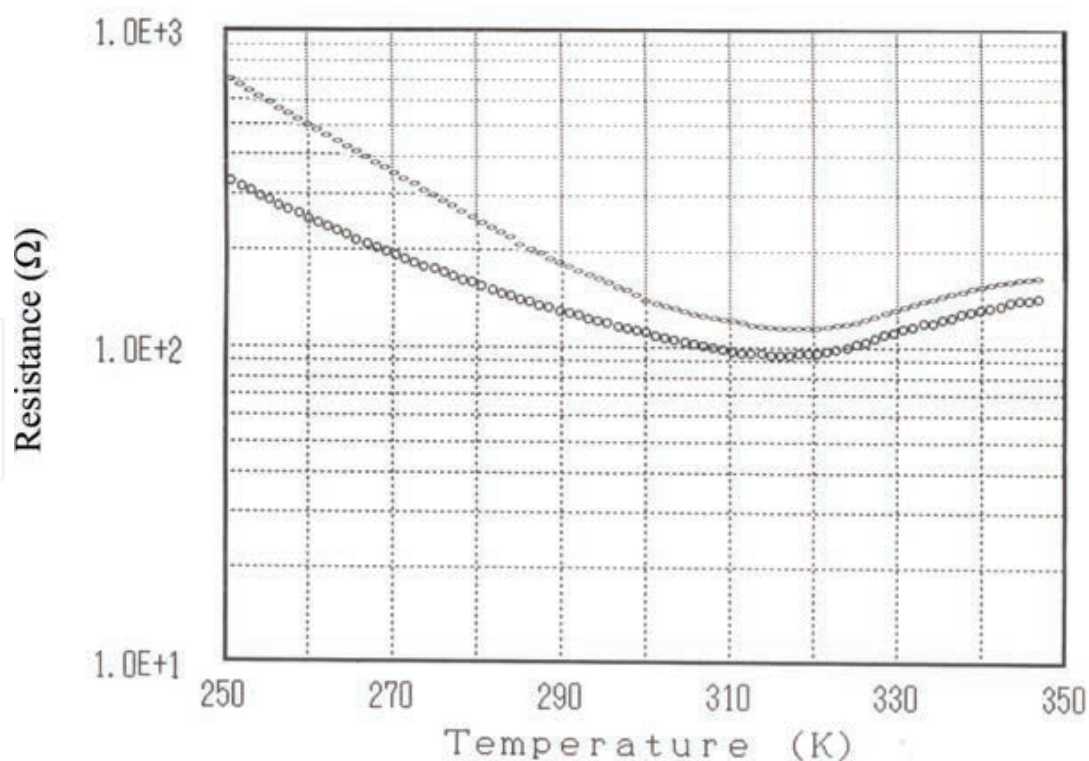


Figure 8. Temperature dependence of resistance of single crystals (EDOB-EDT-TTF)₂AsF₆ in the heating run. Data for two crystals are plotted.

6. Thermoelectric power

Chaikin et al. have described in references [15, 22, 23], that thermoelectric power coefficient in metallic state for a single one-dimensional band is given by:

$$S = \frac{-\pi^2 k_B^2 T}{3|e|} \left(\frac{\cos\left(\frac{\pi\rho}{2}\right)}{2|t|\sin^2\left(\frac{\pi\rho}{2}\right)} + \frac{\tau'(\varepsilon)}{\tau(\varepsilon)_{EF}} \right), \quad (1)$$

where $\tau(\varepsilon)$ is energy-dependent electron scattering time, ρ is amount of charge transfer, t is transfer integral ($4t$ is the bandwidth), k_B is Boltzmann constant, E_F is Fermi energy, and T denotes temperature. When band structure contribution to thermoelectric power dominates in Eq. (1), the sign of thermoelectric power is negative for $\rho < 1$ and positive for $\rho > 1$. S shows linear temperature dependence in metallic region.

Thermoelectric power coefficient for semiconductor is given by:

$$S = \frac{-k_B^2}{|e|} \left(\frac{b-1}{b+1} \frac{E_a}{k_B T} + \ln \frac{m_h}{m_e} \right), \quad (2)$$

where b is the ratio of electron-to-hole mobility, and m_h and m_e are, respectively, effective mass of hole and electron. S shows T^{-1} temperature dependence for semiconductor.

Conwell has shown that near-constant S value close to $-60 \mu\text{V/K}$ over wide temperature range is obtained with model, in which there are strong on-site correlations, U [20, 24].

In this study, thermoelectric power measurements were carried out to clarify MS transition of these salts. Thermoelectric powers of PF_6 , AsF_6 , and SbF_6 salts were measured in temperature range 220–360 K.

6.1. Thermoelectric power of $(\text{EDOB-EDT-TTF})_2\text{PF}_6$

Positive value of thermoelectric power implies hole-like character of conduction charge carriers. The sign (\bullet) of thermoelectric power of PF_6 salt along the crystal growth axis was positive above 235 K as shown in **Figure 9**. Thermoelectric power value of PF_6 salt jumps around 305 and 340 K. Inflection of thermoelectric power curve occurs around 270 K. These jumps and inflection were reproduced for different three samples. Thermoelectric power data (\blacktriangle) measured by Quantum Design PPMS also shows jumps around 272 and 305 K. Thermoelectric power jumps of PF_6 salt shown in **Figure 9** is not clear, however, that of PF_6 salt was proportional to absolute temperature down to 320 K, which is characteristic of metallic conduction. Below 320 K, value of thermoelectric power dropped gradually, indicating MS transition around 320 K. These transition temperatures of PF_6 salt corresponded with the

results of electrical resistivity (\blacktriangledown). Thermoelectric power of PF_6 salt dropped below 305 K, decreasing rapidly below 270 K. Metallic properties denoted both by thermoelectric power and by electrical resistivity measurements.

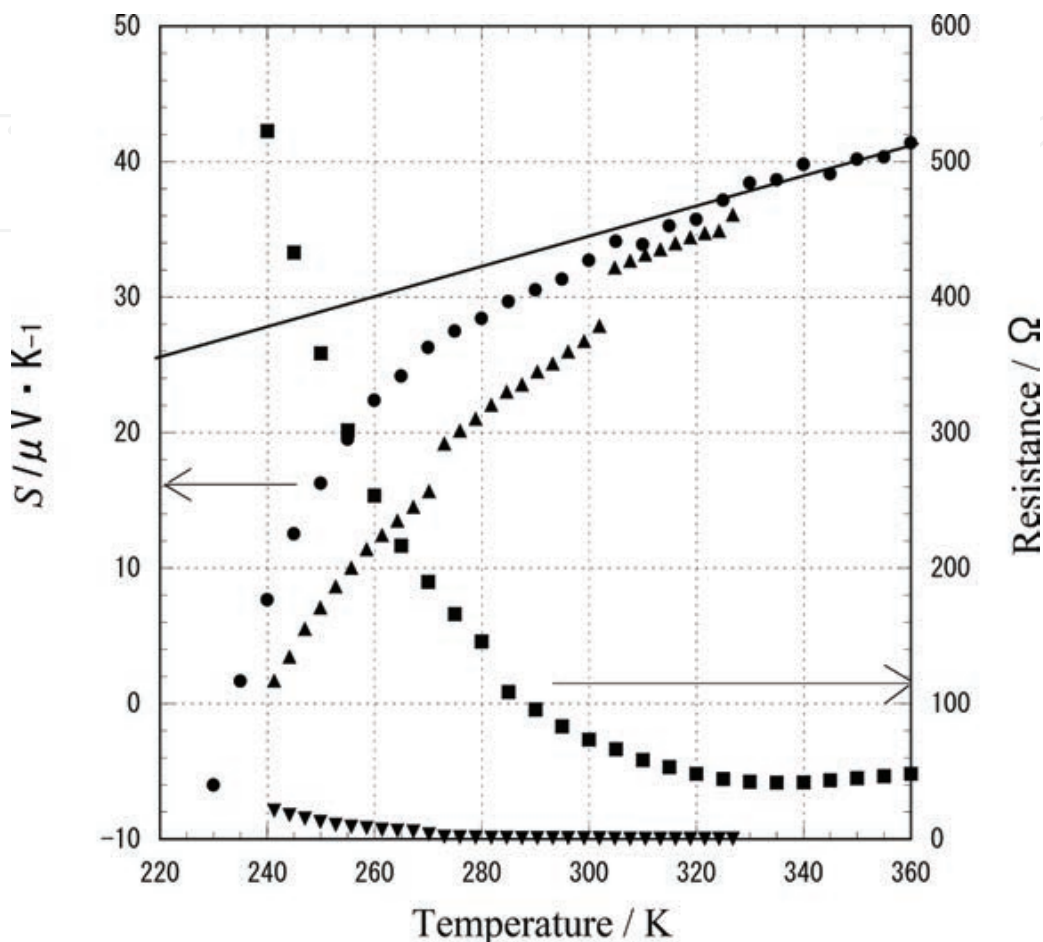


Figure 9. Simultaneous measurements of temperature dependence of thermoelectric power (\bullet) and electrical resistivity (\blacktriangledown) of $(\text{EDOB-EDT-TTF})_2\text{PF}_6$ salt. Data of thermoelectric power (\blacktriangle) and resistivity (\blacktriangledown) were measured by Quantum Design PPMS in temperature range 232–327 K. Solid line extrapolates to zero at $T = 0$ K.

6.2. Thermoelectric power of $(\text{EDOB-EDT-TTF})_2\text{AsF}_6$

Figure 10 shows simultaneous measurements of temperature dependence of thermoelectric power and electrical resistivity of $(\text{EDOB-EDT-TTF})_2\text{AsF}_6$ salt. Thermoelectric power of AsF_6 salt along the crystal growth axis was linear with temperature down to 310 K, which is characteristic of a metal. Thermoelectric power value of AsF_6 salt seems to jump around 305 K and then drops below 300 K, indicating MS transition around 310 K. MS transition temperature observed in thermoelectric power seems to be slightly lower than that of electrical conductivity [25]. Thermoelectric power of AsF_6 salt again showed rapid decrease below 260 K. Inflection of thermoelectric power curve was detected around 260 K. These jumps and inflection were reproduced for different two samples. The sign of thermoelectric power of AsF_6 salt was positive above 220 K. Thermoelectric power of AsF_6 salt became negative below 220 K and

decreased with decreasing temperature. MS transition temperatures of PF_6 and AsF_6 salts observed in thermoelectric power decreased in order of 320 and 310 K.

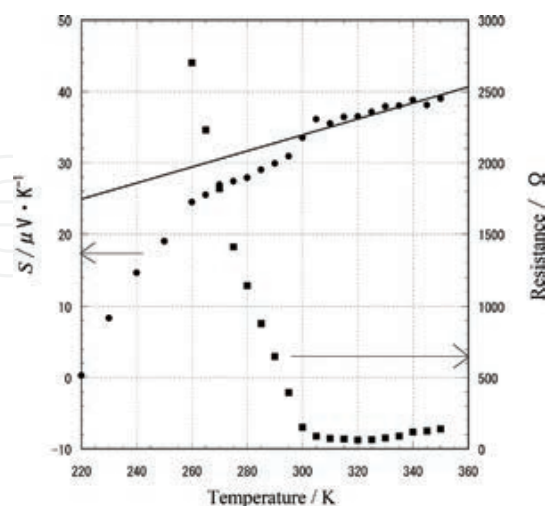


Figure 10. Simultaneous measurements of temperature dependence of thermoelectric power (•) and electrical resistivity (▪) of $(\text{EDOB-EDT-TTF})_2\text{AsF}_6$ salt. Solid line extrapolates to zero at $T = 0$ K.

6.3. Thermoelectric power of $(\text{EDOB-EDT-TTF})_2\text{SbF}_6$

Simultaneous measurements of temperature dependence of thermoelectric power and electrical resistivity of $(\text{EDOB-EDT-TTF})_2\text{SbF}_6$ salt are shown in **Figure 11**. Thermoelectric power value of plate SbF_6 salt was negative below 335 K and decreased with decreasing temperature. Negative value of thermoelectric power implies electron-like character of conduction charge carriers. Thermoelectric power exhibits T^{-1} -temperature dependence, which is a characteristic of semiconductor.

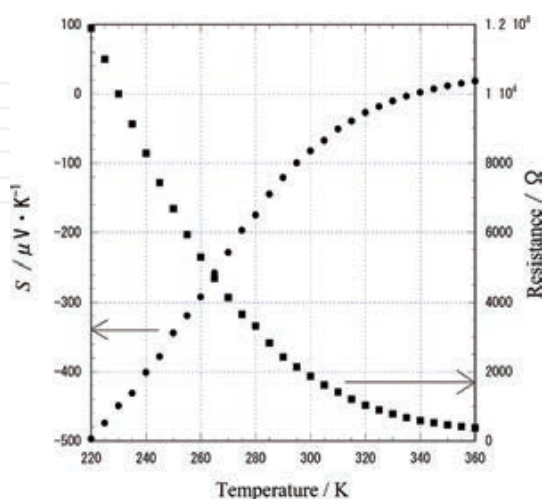


Figure 11. Simultaneous measurements of temperature dependence of thermoelectric power (•) and resistivity (▪) of $(\text{EDOB-EDT-TTF})_2\text{SbF}_6$ salt.

7. Band structure of AsF₆ salt

Band structures of PF₆ and AsF₆ salts were calculated on the basis of tight-binding approximation using intermolecular overlap integrals of HOMO, which were calculated by extended Hückel method [26]. Calculated intermolecular overlap integrals are listed in **Table 3**. Arrangements of donor centers and intermolecular overlaps in EDOB-EDT-TTF salts viewed onto *ab* plane are depicted in **Figure 12**. **Figure 13** shows energy band structures and Fermi surfaces of AsF₆ salt at 293 and 350 K. Energy bands of these salts are three-quarters filled and metallic. Short S...S contacts are observed between stacks, not within the stacks. Such structural feature provides isotropic two-dimensional electronic structures in Fermi surfaces [27, 28].

Symbol	PF ₆ salt at 298 K	AsF ₆ salt at 293 K	AsF ₆ salt at 350 K
S_a	-3.886	-3.864	-3.896
S_{bl}	16.089	12.819	14.467
S_{b2}	12.464	16.414	13.013
S_{p1}	5.545	0.607	5.922
S_{p2}	0.596	5.489	0.605
S_{q1}	0.058	0.058	0.044
S_{q2}	0.056	0.006	0.052

Symbols S_a - S_{q2} represent the overlap integrals between donors shown in **Figure 12**

Table 3. Intermolecular overlap integrals ($\times 10^{-3}$) of EDOB-EDT-TTF salts.

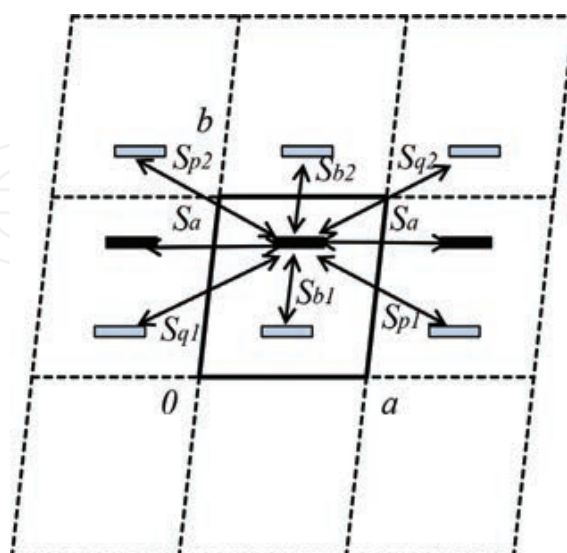


Figure 12. Arrangement of donor centers (,) and intermolecular overlaps in PF₆ salt at 298 K, AsF₆ salts at 293 and 350 K viewed onto *ab* plane.

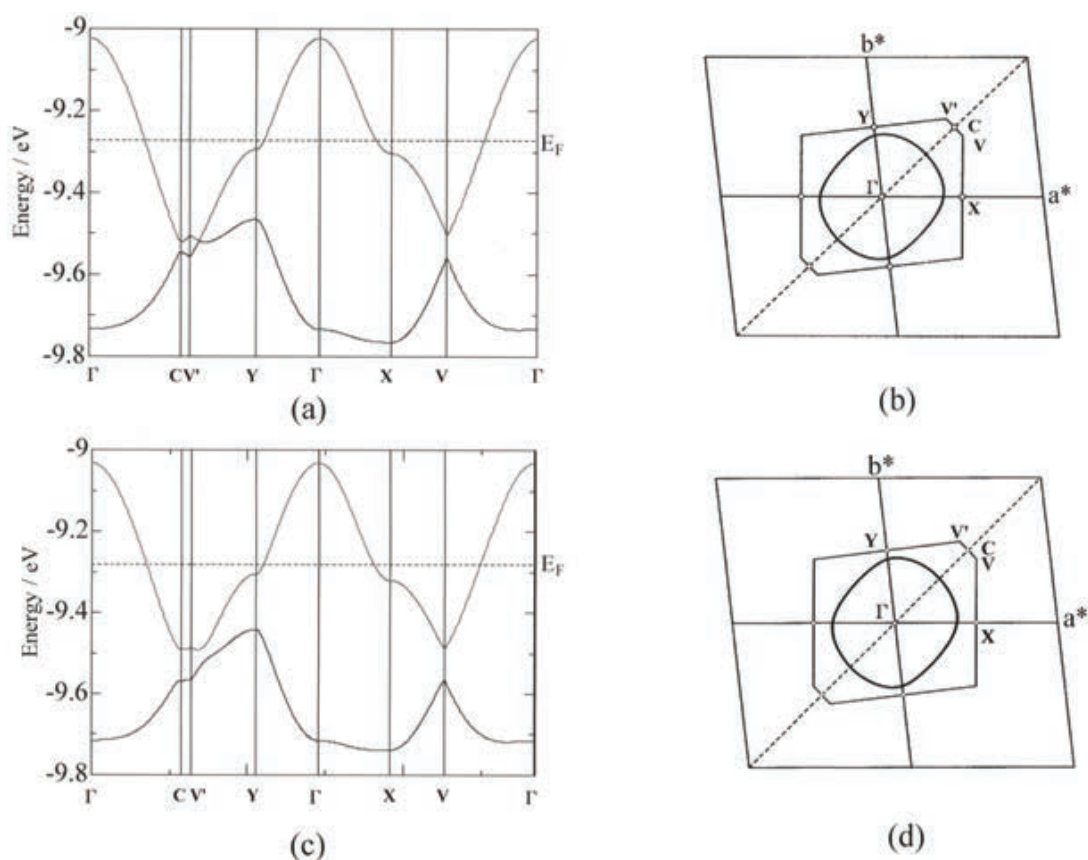


Figure 13. Calculated band structures and corresponding Fermi surfaces of $(\text{EDOB-EDT-TTF})_2\text{AsF}_6$ salt at 293 K (a and b) and 350 K (c and d).

8. Conclusion

Synthesis of unsymmetrical EDOB-EDT-TTF donors was accomplished by two methods. New radical salts with octahedral PF_6^- , AsF_6^- and SbF_6^- anions were prepared by electrochemical oxidation. Crystal structure of AsF_6 salt was isostructural to PF_6 salt, but crystal structure of plate SbF_6 salt was not. According to conventional electrical conductivity measurements, both PF_6 and AsF_6 salts exhibited MS transitions at 340 and 315 K, respectively. Electrical resistivity and thermoelectric power of PF_6 , AsF_6 and SbF_6 salts were measured simultaneously on a single sample. Judging from the results of thermoelectric power measurements, MS transition temperatures of PF_6 and AsF_6 salts were around 320 and 310 K, respectively. From crystal structure analysis in AsF_6 salt follows that intermolecular O...H distance along the stacking b -axis at 350, 330, 293, and 90 K decrease in that order by the dimerization. Formation of dimers results in semiconductor transition. Short S...S contacts were found only between the stacks and not within the stacks. They provided isotropic two-dimensional electronic structure in Fermi surfaces. Two-dimensional electronic structure derived from β -type arrangement is not so stable against packing modification [28]. MS transition is associated with some structural transition.

Acknowledgements

The author wish to thank Drs. Maeda T and Yamashita K of Computer Automation Co. and Dr. Niwa N of System Approach Co. for programming the LabVIEW thermoelectric power measurement system and Emeritus Professor Matsumoto S of Aoyama Gakuin University for giving valuable comments.

Abbreviations

TTF, tetrathiafulvalene; EDT, ethylenedithio; BEDT-TTF, bis(EDT)-TTF; DBTTF, dibenzo-TTF; EDO, ethylenedioxy; BEDO-DBTTF, bis(EDO)-DBTTF; EDOB-EDT-TTF, ethylenedioxybenzo-EDT-TTF; TCNQ, 7,7,8,8-tetracyanoquinodimethane; FTCNQ, 2-fluoro-TCNQ; F₂TCNQ, 2,5-difluoro-TCNQ; Me₂TCNQ, 2,5-dimethyl-TCNQ; TCE, 1,1,2-trichloroethane.

Author details

Tomoko Inayoshi

Address all correspondence to: inayoshi@chem.aoyama.ac.jp

Department of Chemistry and Biological Science, College of Science and Engineering, Aoyama Gakuin University, Sagamihara, Kanagawa, Japan

References

- [1] Coleman L B, Cohen M J, Sandman D J, Yamagishi F G, Garito A F, Heeger A J. Superconducting fluctuations and the peierls instability in an organic solid. *Solid State Commun.* 1973; 12: 1125–732. doi:10.1016/0038-1098(73)90127-0
- [2] Heeger A J, Garito A F. In: Keller H J editor. *Low-Dimensional Cooperative Phenomena*. New York: Plenum Press; 1975. p. 89–124.
- [3] Ishiguro T, Kagoshima S, Anzai H. Dc conductivity anomalies at the transition points in TTF-TCNQ. *J. Phys. Soc. Jpn.* 1976; 41: 351–352. doi:10.1143/JPSJ.41.351
- [4] Kistenmacher T J, Phillips T E, Cowan D O. The crystal structure of the 1:1 cation-radical anion salts of 2,2'-bis-1,3-dithiole (TTF) and 7,7,8,8-tetracyanoquinodimethane (TCNQ). *Acta Cryst.* 1974; B30: 763–768. doi:10.1107/S0567740874003669
- [5] Kwak J F, Chaikin P M, Russel A A, Garito A F, Heeger A J. Anisotropic thermoelectric power of TTF-TCNQ. *Solid State Commun.* 1975; 16: 729–732. doi:10.1016/0038-1098(75)90062-9

- [6] Chaikin P M, Kwak J F. Apparatus for thermopower measurements on organic conductors. *Rev. Sci. Instrum.* 1975; 46: 218–220. doi:10.1063/1.1134171
- [7] Mori T, Inokuchi H. Thermoelectric power of organic superconductors-calculation on the basis of the tight-binding theory. *J. Phys. Soc. Jpn.* 1988; 57: 3674–3677. doi:10.1143/JPSJ.57.3674
- [8] Senga T, Kamoshida K, Kushch L A, Saito G, Inayoshi T, Ono I. Peculiarity of ethylenedioxy group in formation of conductive charge-transfer complexes of bis(ethylenedioxy)-dibenzotetrathiafulvalene (BEDO-DBTTF). *Mol. Cryst. Liq. Cryst.* 1997; 296: 97–143. doi:10.1080/10587259708032316
- [9] Inayoshi T, Matsumoto S, Ono I. Physical properties of CT complexes of a new asymmetric donor: (EDOB)(EDT)TTF. *Synth. Met.* 2003; 133–134: 345–348. doi:10.1016/S0379-6779(02)00334-X
- [10] Inayoshi T, Matsumoto S. Synthesis, electronic properties, thermoelectric power, and crystal and band structures of unsymmetrical EDOB-EDT-TTF salts composed of PF_6^- AsF_6^- SbF_6^- at various temperatures. *Mol. Cryst. Liq. Cryst.* 2013; 582: 136–153. doi:10.1080/15421406.2013.807156
- [11] Mori T, Inokuchi H, Kini A M, Williams J M. Unsymmetrically substituted ethylenedioxytetrathiafulvalenes. *Chem. Lett.* 1990; 19: 1279–1282. doi:10.1246/cl.1990.1279
- [12] Kim G T, Park J G, Lee J Y, Yu H Y, Choi E S, Suh D S, Ha Y S, Park Y W. Simple technique for the simultaneous measurements of the four-probe resistivity and the thermoelectric power. *Rev. Sci. Instrum.* 1998; 69: 3705–3706. doi:10.1063/1.1149164
- [13] Park Y W. Structure and morphology: relation to thermopower properties of conductive polymers. *Synth. Met.* 1991; 45: 173–182. doi:10.1016/0379-6779(91)91801-G
- [14] Barnard R D. *Thermoelectricity in Metals and Alloys*. London: Taylor & Francis; 1972. p. 49.
- [15] Chaikin P M, Kwak J F, Jones T E, Garito A F, Heeger A J. Thermoelectric power tetrathiofulvalinium tetracyanoquinodimethane. *Phys. Rev. Lett.* 1973; 31: 601–604. doi:10.1103/PhysRevLett.31.601
- [16] Mori H. Materials viewpoint of organic superconductors. *J. Phys. Soc. Jap.* 2006; 75: 051003/1–14. doi:10.1143/JPST.75.051003
- [17] Mori T, Kobayashi A, Sasaki Y, Kobayashi H, Saito G, Inokuchi H. Band structure of two types of $(\text{BEDT-TTF})_2\text{I}_3$. *Chem. Lett.* 1984; 13: 957–960. doi:10.1246cl.1984.957
- [18] Bondi A. Van der Waals volumes and radii. *J. Phys. Chem.* 1964; 68: 441–451. doi:10.1021/j100785a001
- [19] Ishiguro T, Yamaji K, Saito G. *Organic Superconductors*. 2nd ed. Berlin: Springer; 1998. p. 125–219.

- [20] Kobayashi H, Mori T, Kato R, Kobayashi A, Sasaki Y, Saito G, Inokuchi H. Transverse conduction and metalinsulator transition in β -(BEDT-TTF)₂PF₆. *Chem. Lett.* 1983; 12: 581–584. doi:10.1246/cl.1983.581
- [21] Senadeera G K R, Kawamoto T, Mori T., Yamaura J, Enoki T. 2 k_F CDW transition in β -(BEDT-TTF)₂PF₆ family salts. *J. Phys. Soc. Jap.* 1998; 67: 4193–4197. doi:10.1143/JPSJ.67.4193
- [22] Chaikin P M, Greene R L, Etemad S, Engler E M. Thermopower of an isostructural series of organic conductors. *Phys. Rev.* 1976; B13, 1627–1632. doi:10.1103/PhysRevB.13.1627
- [23] Chaikin P M, Kwak J F, Greene R L, Etemad S, Engler E M. Two band transport and disorder effects in a series of organic alloys: (TTF_{1-x}TSeF_x)-TCNQ (tetrathiafulvalene-tetraselenafulvalene-tetracyanoquinodimethane). *Solid State Commun.* 1976; 19: 1201–1204. doi:10.1016/0038-1098(76)90819-X
- [24] Conwell E M. Thermoelectric power of 1:2 tetracyanoquinodimethanide (TCNQ) salts. *Phys. Rev.* 1978; B18: 1818–1823. doi:10.1103/PhysRevB.18.1818
- [25] Kikuchi K, Saito K, Ikemoto I, Murata K, Ishiguro T, Kobayashi K. Physical properties of (DMET)₂X. *Synth. Met.* 1988; 27: 269–274. doi:10.1016/0379-6779(88)90155-5
- [26] Mori T, Kobayashi A, Sasaki Y, Kobayashi H, Saito G, Inokuchi H. The intermolecular interaction of tetrathiafulvalene and bis(ethylenedithio)tetrathiafulvalene in organic metals. Calculation of orbital overlaps and models of energy-band structures. *Bull. Chem. Soc. Jpn.* 1984; 57: 627–633. doi:10.1246/bcsj.57.627
- [27] Wosnitza J. *Fermi Surfaces of Low-Dimensional Organic Metals and Superconductors.* Berlin: Springer; 1996. p. 34.
- [28] Kagoshima S, Kato R, Fukuyama H, Seo H, Kino H. Chapter 4 Interplay of structural and electronic properties. In: Bernier P, Lefrant S, Bidan G, editors. *Advances in Synthetic Metals—Twenty Years of Progress in Science and Technology.* Amsterdam: Elsevier; 1999. p. 262–316.

IntechOpen

